JOURNAL OF SOLID STATE CHEMISTRY 85, 133–143 (1990)

Short-Range Order in the Anion-Excess Fluorite-Related $Ca_{0.68}Ln_{0.32}F_{2.32}$ Solid Solutions: EXAFS Study of the Ln^{3+} Environment

J. P. LAVAL, A. ABAOUZ, AND B. FRIT*

Laboratoire de Chimie Minérale Structurale, UA–CNRS No. 320, Faculté des sciences de Limoges, 123 Avenue A. Thomas, 87060 Limoges Cedex, France

AND A. LE BAIL

Laboratoire des Fluorures, UA–CNRS No. 449, Université du Maine, 72017 Le Mans Cedex, France

Received August 21, 1989

Anion-excess fluorite-type $Ca_{0.68}Ln_{0.32}F_{2.32}$ series and Ca_2LnF_7-related low-temperature superstructures were studied by EXAFS. This analysis, completed with a structure refinement of Ca_2LuF_7, shows the narrow analogy between clustering in ordered and disordered states. It confirms the change in short-range order when Ln^{3+} size increases, as previously evidenced by a neutron diffraction study.

I. Introduction

A recent powder neutron diffraction study of the $Ca_{0.68}Ln_{0.32}F_{2.32}$ series (Ln = La, Nd, Tb, Ho, Er, Yb, Lu) clearly indicated a steady evolution of the defect structure (*1*). With increasing dopant cation size, F′ interstitials (1/2,x,x; x = 0.37) prominent for small cations (Lu, Yb) are progressively replaced by F″ interstitials (x,x,x; x = 0.41) and relaxed normal fluorine F‴ atoms (x,x,x; x = 0.31). These results can be explained by the presence of large dopant cations (La–Tb) in small 1:0:3 clusters (one vacancy, 0 F′ and 3 F″) involving two ninefold coordinated Ln^{3+} cations, and of small and medium dopant cations (Ho–Lu) in a mixture of small 1:0:3 clusters and large cuboctahedral 8:12:1 clusters (eight vacancies, 12 F′, 1 F″), the number of the latter increasing with the decrease of the dopant cation size. The results of previous neutron diffraction studies (*2, 3*) support a change in cluster structure with dopant cation radius, showing significant differences between defect structures in La-doped CaF_2 and Er-doped CaF_2. However, diffraction gives only average structural information; in contrast, Extended X-ray Absorption Fine Structure (EXAFS) provides information on the local structural environment of individual atom types (i.e., dopant cations) and therefore should give direct evidence for such a change in cluster struc-

* To whom correspondence should be addressed.

0022-4596/90 $3.00

ture. Using this technique to study the $Ca_{0.9}Ln_{0.1}F_{2.1}$ (Ln = La, Pr, Nd, Gd, Tb, Dy, Ho, Er, Tm, Yb) series Catlow *et al.* (*4*) have observed the way by which the local structural environment of the dopant cation is altered with the size of this rare-earth ion. We have therefore undertaken an EXAFS study of the $Ca_{0.68}Ln_{0.32}F_{2.32}$ series.

Low-temperature fluorite-related superstructures with the composition Ca_2LnF_7 ($MX_{2.33}$), very close to that of the samples samples studied ($MX_{2.32}$), are known for the heaviest rare-earths (Ln = Lu–Ho) (*5*). Their thermal stability decreases with increasing Ln^{3+} size. The recent structural determination of Ca_2YbF_7 (*6, 7*) provides a basis for a comparison with the disordered phases. In the present work, the structure of the isomorphic Ca_2LuF_7 phase has been refined from X-ray powder diffraction data in order to obtain another set of structural data. These materials together with Ca_2ErF_7 and LnF_3 (Ln = Lu, Yb, Er, Ho, Tb) were used as references for the EXAFS study.

II. Experimental

The samples of Ca_2LnF_7 (Ln = Lu, Yb, Er) were prepared by heating for 2 days at 1073 K the intimate mixtures ($2CaF_2$, LnF_3) in sealed platinum tubes, and then cooling to 773 K in steps of 50 K and 3 days each. After grinding, the powders were annealed again for 2 weeks at 773 K. The disordered samples were prepared as in (*1*).

The X-ray diffraction spectrum of Ca_2LuF_7 was recorded in the range $10 < 2\theta < 126°$ in steps of 0.04° with a back monochromatized Cu$K\alpha$ Siemens D500 diffractometer.

The EXAFS spectra were recorded at 30 K for the L_{III} absorption edge of Ln atoms, using synchrotron radiation at LURE. The monochromator was a channel-cut silicon the beam realized by ionization cameras located in front of and behind the sample. Finely ground powder was regularly dispersed on sticky tape.

The data were analyzed by using a procedure previously described (*8, 9*) which can be summarized briefly in the following steps:

—determination of the EXAFS modulations $X(k)$ which were weighted by a k^3 factor.

—evaluation of the modulus $|F(R)|$ of the Fourier transform of $f(k) = k^3 \cdot X(k)$.

—when possible, estimation of the partial function $f_j(k)$, associated with the coordination sphere of order j, by an inverse Fourier transform of $F(R)$ in a selected interval $(R_{min}, R_{max})_j$.

The filtered spectra were approximated by the relation of Stern *et al.* (*10*). Theoretical amplitudes and phase shifts calculated by Teo and Lee (*11*) have been used to fit the spectra. For testing the Teo and Lee parameters, R_j (mean radius of the coordination sphere), σ_j (relative root mean square displacement from R_j due to thermal and static disorder), and S_0^2 (multielectronic factor used as a scaling factor for a given number of backscattering centers N_j) were refined by a least-squares method in the case of reference materials, with the value of the edge energy E_0 adjusted to the best fit.

III. Results

1. LnF_3 Reference Materials

$|F(R)|$ for LnF_3 materials are represented in Fig. 1. The HoF_3 spectrum was also recorded at room temperature and the comparison with the results at 30 K shows clearly that reducing the temperature considerably improves the quality of the spectrum. These rare-earth trifluorides are iso-

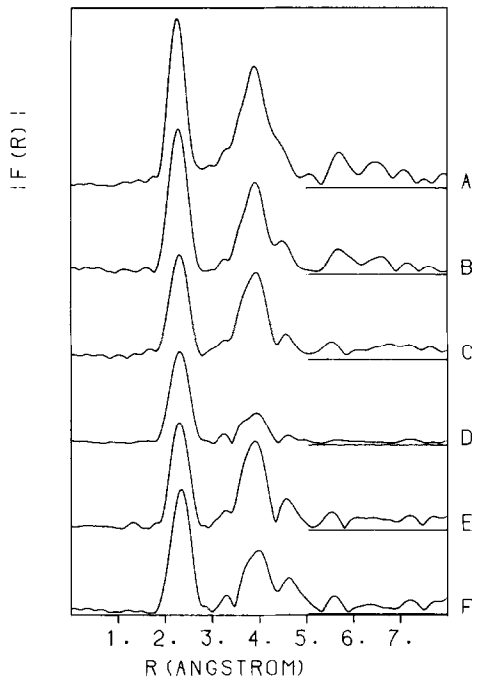

Fig. 1. Fourier transforms of the EXAFS spectra at 30 K for the LnF_3 references, corrected for (Ln–F) phase shift: A = LuF_3, B = YbF_3, C = ErF_3, D = HoF_3 (293 K), E = HoF_3, F = TbF_3.

carried out only for β-SmF_3, HoF_3, and β-YbF_3 (*14*). The *Ln* coordination may be considered as [8 + 1], the last fluorine atom clearly being at a longer distance. EXAFS results are summarized in Table I. They are in good agreement with the structural data provided that the mean $\langle Ln\text{–F}\rangle$ distance is calculated from the eight nearest F neighbors. A simulation of the contribution of next nearest neighbors was not attempted. The intense and broad peak on $|F(R)|$ is presumably dominated by *Ln–Ln* pairs; however, in HoF_3, for instance, five different types of Ho–Ho distances between 3.606 and 4.376 Å are present.

2. Ca_2LnF_7 Reference Materials

(*a*) *Structure Refinement of* Ca_2LuF_7

Refinements were performed using a modified Rietveld method (*15*) starting from the Ca_2YbF_7 coordinates (*6, 7*) in the space group *I*4/*m* (a = 8.6633(3) Å, c = 16.5252(8) Å, Z = 10). The conventional Rietveld reliability factors converged rapidly to R_i = 0.050, R_p = 0.092, and R_{wp} = 0.103 for 27 refined structural parameters and 521 reflections. Table II reports the refined structural parameters and the main interatomic distances; the coordinates remain very close to the Ca_2YbF_7 values, the same partial cationic disorder being observed.

A projection of the Ca_2LuF_7 structure onto the (001) plane is shown in Fig. 2. This superstructure of the fluorite-type can be described as an ordered distribution of Ca Lu_5F_{37} clusters of six corner-sharing square antiprisms enclosing a cuboctahedron of anions, with this cuboctahedron containing an additional anion at its center. These clusters are identical to the 8 : 12 : 1 ones used for the modeling of the $Ca_{0.68}Ln_{0.32}F_{2.32}$ (*Ln* = Ho–Lu) defect structure. Two kinds of intercationic distances can be distinguished:

—"long" distances ($\langle$4.09 Å$\rangle$) between cations (mainly Lu–Lu pairs) located at the center of two adjacent square antiprims sharing a corner within the cuboctahedral cluster.

—"short" distances ($\langle$3.79 Å$\rangle$) between cations (mainly Ca–Ca and Lu–Ca pairs) located at the center of two adjacent polyhedra sharing an edge or a face.

The subsequent distortion of the fcc cationic subcell (expansion of the lanthanide network inside the cuboctahedral cluster) is clearly shown by the schematic projection in Fig. 3. This discrepancy between "long" and "short" intercationic distances is still more obvious when weighted averages of these distances around a given Ln^{3+} cation are considered. Those reported in Table III show that this phenomenon has a general character since it is observed for all the known fluorite-related superstructures containing the same cuboctahedral clusters, even when these clusters are isolated as in tveitite (*18, 19*).

TABLE I

CRYSTALLOGRAPHIC DATA (ROOM TEMPERATURE) AND EXAFS PARAMETERS (30 K) FOR REFERENCE MATERIALS

Compound	Distances	X-ray weighted average values		EXAFS R(Å)	EXAFS σ(Å)	EXAFS S_0^2	N
LuF_3	Lu–F	—	—	2.23	0.027	0.317	8 + 1
YbF_3	Yb–F	2.30	(2.26)[a]	2.26	0.043	0.363	8 + 1
ErF_3	Er–F	—	—	2.28	0.052	0.291	8 + 1
HoF_3 (293 K)	Ho–F	2.32	(2.30)[a]	2.29	0.077	0.353	8 + 1
HoF_3				2.29	0.046	0.297	
TbF_3	Tb–F	—	—	2.32	0.043	0.349	8 + 1
Ca_2LuF_7	Lu–F		2.28	2.22	0.069	0.370	8 + 1
	Lu–(Ca, Lu) intracluster	4.09	—	4.10	0.090	0.525	4
	Lu–(Ca, Lu) extracluster	3.79	—	3.76	0.082	0.269	8
Ca_2YbF_7	Yb–F		2.26[a]	2.23	0.077	0.386	8 + 1
	Yb–(Ca, Yb) intracluster	4.10	—	4.15	0.086	0.467	4
	Yb–(Ca, Yb) extracluster	3.80	—	3.78	0.086	0.273	8
Ca_2ErF_7	Er–F	—	—	2.24	0.079	0.309	8 + 1
	Er–(Ca, Er) intracluster	—	—	4.18	0.089	0.427	4
	Er–(Ca, Er) extracluster	—	—	3.79	0.076	0.163	8

[a] Values for eightfold coordination.

TABLE IIA

REFINED STRUCTURAL PARAMETERS FOR Ca_2LuF_7

Atom	Site	x	y	z	B(Å^2)	Occupation[a]
Ca(1)	16*i*	0.3849(6)	0.1944(7)	0.1633(3)	0.34(9)	0.994(4)
Ca(2)	2*b*	0	0	1/2	0.2(1)	0.87(1)
Lu(1)	8*h*	0.1076(3)	0.3106(3)	0	0.44(5)	0.78(1)
Lu(2)	4*e*	0	0	0.1804(2)	0.55(8)	0.78(1)
F(1)	16*i*	0.292(2)	0.421(1)	0.0760(6)	1.5(1)	1[b]
F(2)	16*i*	0.082(2)	0.228(1)	0.1278(7)		
F(3)	8*h*	0.304(2)	0.155(2)	0		
F(4)	8*g*	0	1/2	0.0811(9)		
F(5)	2*a*	0	0	0		
F(6)	16*i*	0.296(2)	0.400(1)	0.2383(6)		
F(7)	4*d*	0	1/2	1/4		

[a] All cationic sites are fully occupied by a mixture of Ca,Lu; the occupation rate is given for the dominant cation in the site, e.g., Ca(1),Ca(2),Lu(1),Lu(2).

[b] Fixed values. The theoretical occupancy for Lu(1) and Lu(2) sites is 0.833 (5/6 Lu and 1/6 Ca). So the cationic ordering is incomplete: 22% Ca is present on Lu sites and conversely 13% Lu on the Ca(2) site (cubic site). The global refined cationic proportion is $Ca_{2.028}Lu_{0.972}$.

TABLE IIB

MAIN INTERATOMIC DISTANCES FOR Ca_2LuF_7

Ln–F	*Ln*(1)–F(3)	2.17(2)	
2×	*Ln*(1)–F(2)	2.24(1)	
2×	*Ln*(1)–F(1)	2.25(1)	Square antiprism [8 + 1]
	Ln(1)–F(3)	2.28(2)	
2×	*Ln*(1)–F(4)	2.32(1)	
	Ln(1)–F(5)	2.85(2)	
4×	*Ln*(2)–F(2)	2.27(1)	
4×	*Ln*(2)–F(6)	2.38(1)	Square antiprism [8 + 1]
	Ln(2)–F(5)	2.98(1)	
Ca–F	$Ca(1)_2$–F(6)	2.30(1)	
	$Ca(1)_2$–F(1)	2.37(1)	
	$Ca(1)_2$–F(4)	2.38(1)	
	$Ca(1)_2$–F(6)	2.40(1)	
	$Ca(1)_2$–F(6)	2.41(1)	"Centaur" polyhedron [7 + 3]
	$Ca(1)_2$–F(7)	2.43(1)	
	$Ca(1)_2$–F(1)	2.57(1)	
	$Ca(1)_2$–F(2)	2.71(1)	
	$Ca(1)_2$–F(3)	2.81(1)	
	$Ca(1)_2$–F(2)	2.82(1)	
8×	Ca(2)–F(1)	2.30(1)	Cube [8]
M–M			
Corner-sharing polyhedra	*Ln*(1)–$Ln(1)_1$	4.027(4)	
	Ln(1)–*Ln*(2)	4.123(3)	
	Ln(1)–$Ln(1)_2$	3.774(4)	
	Ln(1)–$Ca(1)_3$	3.848(6)	
	Ln(1)–Ca(2)	3.775(3)	
	Ln(2)–$Ca(1)_4$	3.831(6)	
Edge-sharing polyhedra	$Ca(1)_1$–$Ca(1)_4$	3.821(7)	
	$Ca(1)_1$–$Ca(1)_3$	4.001(8)	
	$Ca(1)_2$–$Ca(1)_3$	3.914(9)	
	$Ca(1)_3$–$Ca(1)_4$	3.984(7)	
	$Ca(1)_1$–Ca(2)	3.910(6)	
Face-sharing polyhedra	*Ln*(1)–$Ca(1)_1$	3.751(6)	
	Ln(1)–$Ca(1)_2$	3.813(6)	
	Ln(2)–$Ca(1)_1$	3.746(6)	

Therefore, the presence of such clusters, disordered or not, within a fluorite matrix should be detectable by an EXAFS study.

(b) EXAFS Study of Ordered Ca_2LnF_7 Phases

$|F(R)|$ for the ordered Ca_2LnF_7 (*Ln* = Lu, Yb, Er) phases are shown in Fig. 4. The first main peak corresponds to *Ln*-F first neighbors; then, two separate peaks are defined between 3.0 and 5.0 Å. They were attributed to the "short" and "long" distances mentioned above, having been verified by simulations that:

—the influence of second F neighbors is negligible (due to the rapid decreasing of their backscattering amplitude with k compared to that of Ca and *Ln*, this effect being accentuated by the higher thermal motion of F).

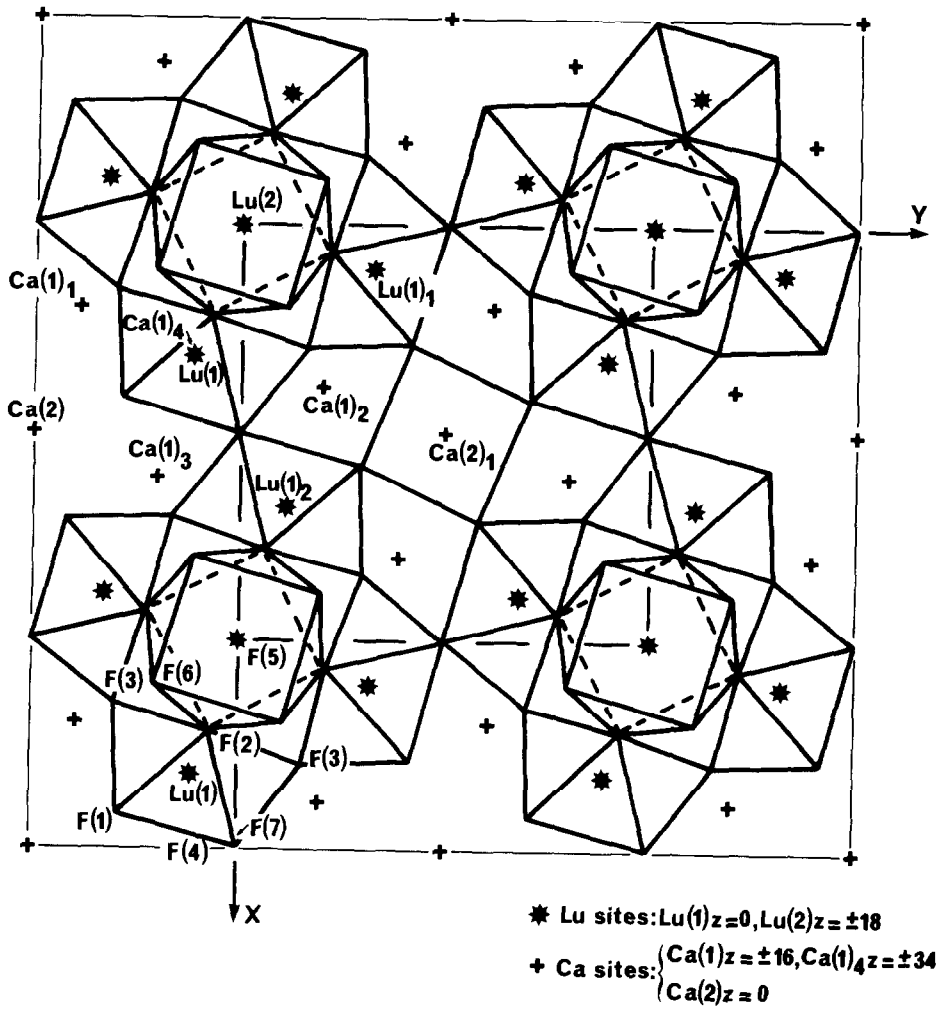

Fig. 2. A basic sheet in Ca_2LuF_7 projected onto the (001) plane.

—a separation between *Ln*–Ca and *Ln*–*Ln* contributions on $|F(R)|$ exists, even when the distances are the same, due to a backscatterer phase shift effect (i.e., the peaks move by a value of −0.4 Å from the theoretical position for *Ln*–Ca and only of −0.15 Å for *Ln*–*Ln*).

Taking into account these considerations, the two peaks were separately fitted as *Ln*–Ca and *Ln*–*Ln* contributions, neglecting the partial cationic disorder. Despite these approximations, interatomic distances (Table I) are in good accord with the experimental values resulting from X-ray diffraction studies.

3. Disordered Phases

Figure 5 presents the Fourier-transformed EXAFS spectra $|F(R)|$ of the $Ca_{0.68}Ln_{0.32}F_{2.32}$ phases. The first main peak obviously corresponds to *Ln*–F first neighbors; as in the ordered phases the two next peaks were tentatively attributed to *Ln*–Ca and *Ln*–*Ln* respectively. This hypothesis was supported by the good quality of the

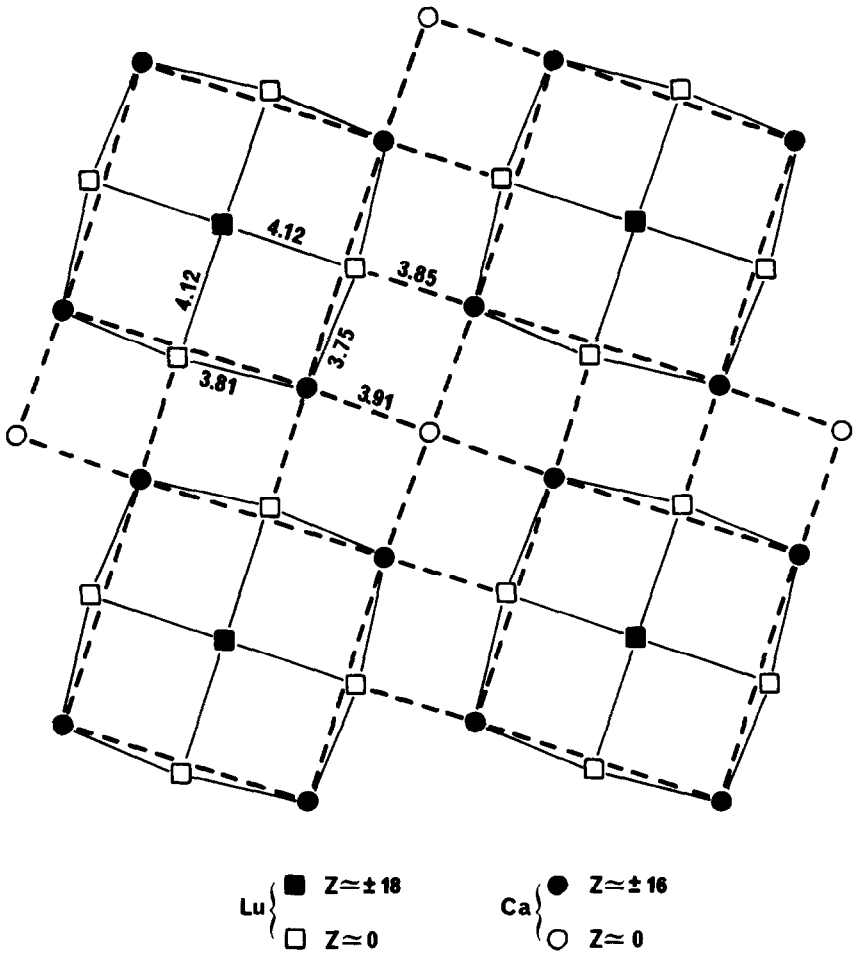

Fig. 3. Schematic projection onto (001) of the distorted fcc cationic subcell in Ca_2LuF_7.

fits. The main results deduced from the EXAFS analysis are reported in Table IV.

IV. Discussion and Conclusion

From Table IV, two general observations can be made:

—the regular increase in interatomic distances from Lu to Tb compounds, in direct correlation with the rare-earth ionic radius increase;

—the nearly perfect identity of interatomic distances between ordered and disordered homologous phases, which indicates the great analogy of their structure.

From the EXAFS intercationic distances, a weighted average was calculated supposing, as in the Ca_2LnF_7-ordered superstructures, an ideal distribution: 8/12 of *Ln*–Ca and 4/12 of *Ln*–*Ln* distances. These values are compared in Table IV to the statistical (Ca, *Ln*)–(Ca, *Ln*) distances obtained by neutron diffraction structure determination (*1*). The agreement is rather good, except for *Ln* = Tb. This adequately supports the peak attribution used for the EXAFS interpretation, but clearly the Tb phase is an exception.

From the previous neutron study (see the Introduction), it was concluded that the

TABLE III

WEIGHTED AVERAGE INTERCATIONIC DISTANCES AROUND A GIVEN Ln^{3+} CATION OF A CUBOCTAHEDRAL CLUSTER FOR VARIOUS ANION-EXCESS FLUORITE-RELATED SUPERSTRUCTURES

	Compounds				
Ln–cation (Å)	Ca_2LuF_7	Ca_2YbF_7 (*7*)	$Na_7Zr_6F_{31}$ (*16*)	KY_3F_{10} (*17*)	Tveitite (*18, 19*)
"Long" distances					
Inside cluster	4.09	4.10	4.09	4.24	4.13
"Short" distances					
Between clusters	3.77	3.76	3.65	3.92	—
Between cluster and outside	3.79	3.80	3.81	4.08	3.80

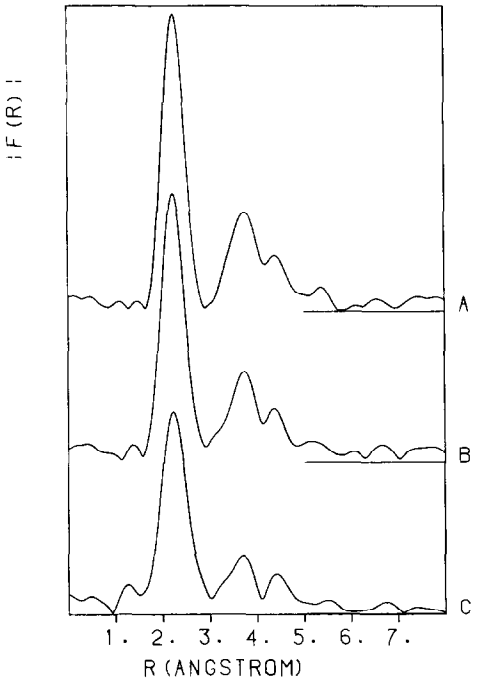

Fig. 4. Fourier transforms of the EXAFS spectra at 30 K for the Ca_2LnF_7 references, corrected for (*Ln*–F) phase shift. A = Ca_2LuF_7, B = Ca_2YbF_7, C = Ca_2ErF_7.

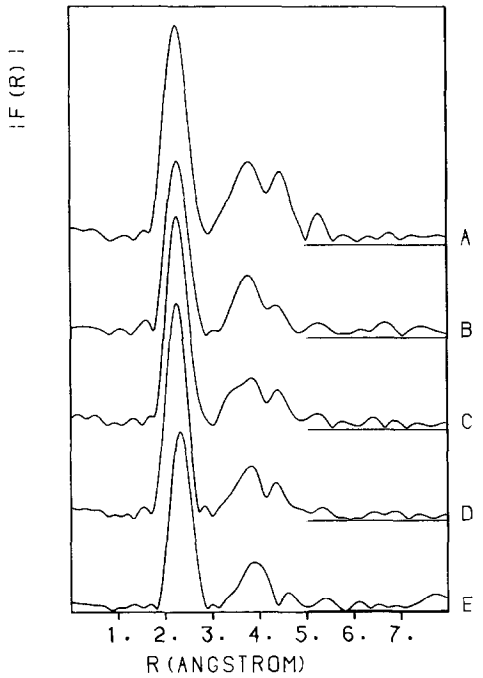

Fig. 5. Fourier transform of the EXAFS spectra at 30 K for the $Ca_{0.68}Ln_{0.32}F_{2.32}$ phases corrected for (*Ln*–F) phase shift. *Ln* = Lu (A), Yb (B), Er (C), Ho (D), Tb (E).

TABLE IV

EXAFS PARAMETERS FOR DISORDERED $Ca_{0.68}Ln_{0.32}F_{2.32}$ AND ORDERED Ca_2LnF_7 PHASES: COMPARISON WITH STRUCTURAL RESULTS (X-RAY OR NEUTRON DIFFRACTION)

Distances in (Å) $CaF_2:Ln^{3+}$	EXAFS				Neutrons		X-Ray			
								(Ca, *Ln*)–(Ca, *Ln*)		
	Ln–Ca	*Ln*–*Ln*	*Ln*–F	⟨*Ln*–(Ca, *Ln*)⟩	(Ca, *Ln*)–(Ca, *Ln*)	(Ca, *Ln*)–F	*Ln*–F	Extracluster	Intracluster	Average
Lu										
Disordered	3.77	4.12	2.22	3.89	3.88	–F′ : 2.12 ⟨2.25⟩ –F : 2.37	—	—	—	—
Ordered	3.76	4.10	2.22	3.87	—	—	Lu(1)–F : 2.26 Lu(2)–F : 2.32 ⟨2.28⟩	3.79	4.09	3.89
Yb										
Disordered	3.79	4.16	2.23	3.91	3.89	–F′ : 2.14 ⟨2.26⟩ –F : 2.38		—	—	—
Ordered	3.78	4.15	2.23	3.90	—	—	Yb(1)–F : 2.26 Yb(2)–F : 2.25 ⟨2.26⟩	3.80	4.10	3.90
Er										
Disordered	3.83(3.93)[a]	4.16(4.21)[a]	2.25(2.35)[a]	3.94	3.90	–F′ : 2.15 ⟨2.27⟩ –F : 2.39	—	—	—	—
Partly ordered	3.79	4.18	2.24	3.92	—	—	—	—	—	—
Ho										
Disordered	3.85	4.17	2.27	3.96	3.91	–F′ : 2.16 ⟨2.28⟩ –F : 2.39	—	—	—	—
Tb										
Disordered	3.94	4.28	2.31	4.05	3.92	–F″ : 2.39 ⟨2.40⟩ –F : 2.40	—	—	—	—

[a] Ref (*4*).

cuboctahedral clusters are progressively replaced from Lu to Tb by small 1 : 0 : 3 clusters. If the EXAFS interpretation of cuboctahedral clusters only is assumed, the failure of this model for Tb confirms the change in the short-range order. A more complicated modeling of the EXAFS modulations would be unreasonable.

In another way, the neutron (Ca, *Ln*)–F distances are anomalous (in particular, the (Ca, *Ln*)–F′ is too short), reflecting the fact that the *Ln* cation subnetwork inside the cuboctahedral clusters is probably expanded as in Ca_2LnF_7–ordered phases (Fig. 3).

Although unable to give a direct picture of the defect structure in these $Ca_{0.68}Ln_{0.32}F_{2.32}$ series, this EXAFS study is in accordance with the previously proposed defect structure model.

All these results lead essentially to the same conclusions as those of previous lattice simulation (*20*), neutron diffraction (*2, 3*), and EXAFS (*4*) studies on a much less doped $Ca_{0.90}Ln_{0.10}F_{2.10}$ series. For these last phases, the authors proposed the substitution of large cuboctahedral clusters for small "dimers" with decreasing dopant cation size. However, the "dimer" cluster proposed (*2, 3*) is different from the 1 : 0 : 3 cluster.

Our studies strongly suggest that the nature of short-range order in anion-excess fluorite-related $Ca_{1-x}Ln_xF_{2+x}$ solid solution is highly dependent on the size and the coordination of the Ln^{3+} dopant cation. When 9- or 10-fold coordination is geometrically possible, small 1 : 0 : 3 clusters are the most stable defects. With decreasing Ln^{3+} radius, 8-fold coordination is favored and 8 : 12 : 1 clusters become more stable. Their increasing rate leads to long-range ordering at low temperature and then to M_nF_{2n+5} superstructures (*18*). For Ln^{3+} cations of medium size (Er^{3+}, Ho^{3+}, and also Y^{3+}), a mixture of both 1 : 0 : 3 and 8 : 12 : 1 clusters is probably observed, although the presence of intermediate clusters, precursors of the 8 : 12 : 1 cluster, like the 4 : 4 : 3 clusters previously proposed for the $Ca_{1-x}Y_xF_{2+x}$ solid solution (*21*), cannot be excluded.

A study of the evolution of equilibrium conditions among these various clusters under temperature and annealing conditions would surely be of value.

Note added in proof. As we were about to submit this paper we received from Professor Bärnighausen in Karlsruhe a copy of the Doctoral Dissertation of A. Lumpp (*22*). This work describes the structural determination of Nd_3Cl_7, a compound which is essentially isostructural with Ca_2YbF_7 and Ca_2LuF_7.

References

1. J. P. Laval, A. Mikou, B. Frit, and G. Roult, *Solid State Ionics*, **28–30,** 1300 (1988).
2. C. R. A. Catlow, A. V. Chadwick, and J. Corish, *Radiat. Eff.* **75,** 61 (1983).
3. C. R. A. Catlow, A. V. Chadwick, and J. Corish, *J. Solid State Chem.* **48,** 65 (1983).
4. C. R. A. Catlow, A. V. Chadwick, G. N. Greaves, and L. M. Moroney, *Nature (London)* **312,** 601 (1984).
5. O. Greis and M. Kieser, *Z. Anorg. Allg. Chem.* **479,** 165 (1981).
6. S. E. Ness, D. J. M. Bevan, and H. J. Rossell, *Eur. J. Solid State Inorg. Chem.* **25,** 509 (1988).
7. D. J. M. Bevan, M. J. McCall, S. E. Ness, and M. R. Taylor, *Eur. J. Solid State Inorg. Chem.* **25,** 517 (1988).
8. A. Le Bail, C. Jacoboni, and R. De Pape, *J. Solid State Chem.* **52,** 32 (1984).
9. F. Studer, A. Le Bail, and B. Raveau, *J. Solid State Chem.* **63,** 414 (1986).
10. E. A. Stern, B. A. Bunker, and S. M. Heald, *Phys. Rev.* **321,** 5521 (1980).
11. B. K. Teo and P. A. Lee, *J. Amer. Chem. Soc.* **101,** 2815 (1979).
12. A. Zalkin and D. H. Templeton, *J. Amer. Chem. Soc.* **75,** 2453 (1953).
13. A. K. Cheetham and N. Norman, *Acta Chem. Scand. A* **28,** 55 (1974).
14. B. V. Bukvetskii and L. S. Garashina, *Koord. Khim.* **3,** 1024 (1977).

15. A. Le Bail, H. Duroy, and J. L. Fourquet, *Mater. Res. Bull.* **23,** 447 (1988).
16. J. H. Burns, R. D. Ellison, and H. A. Levy, *Acta Crystallogr. B* **24,** 230 (1968).
17. J. W. Pierce and H. Y. P. Hong, *Proc. Rare Earth Res. Conf. 10th, A* **2,** 527 (1973).
18. D. J. M. Bevan, O. Greis, and J. Strähle, *Acta Crystallogr. A* **36,** 889 (1980).
19. D. J. M. Bevan, J. Strähle, and O. Greis, *J. Solid State Chem.* **44,** 75 (1982).
20. J. Corish, C. R. A. Catlow, P. W. M. Jacobs, and S. H. Ong, *Phys. Rev., B* **25,** 6425 (1982).
21. J. P. Laval and B. Frit, *J. Solid State Chem.* **49,** 237 (1983).
22. A. Lumpp, Doctoral dissertation, Karlsruhe University, ISBN 3.923161.21.2 (1988).